SIN-CHN SCIENTIFIC PRESS PTE.LTD.

*Molecular & Cellular Biomechanics* 2024, 21(3), 388.
https://doi.org/10.62617/mcb388

Article

# Exploring the mechanism of Danggui Buxue decoction against acute renal insufficiency using network pharmacology and molecular docking

**Xiaoyue Lou[1], Yongfeng Ma[1], Jiuling Deng[2], You Lv[1], Runhua Li[1], Mingli Shang[1], Qianwen Zhang[1], Xiuling Zhang[2,*], Tingting Hou[1,*]**

[1] College of Pharmacy, Sanquan College of Xinxiang Medical University, Xinxiang 453003, China
[2] Department of Pharmacy, Shanghai Fifth People's Hospital, Fudan University, Shanghai 200240, China
*** Corresponding authors:** Tingting Hou, Email944481621@qq.com; Xiuling Zhang, Emailwww.xiuling@163.com

**CITATION**

Lou X, Ma Y, Deng J, et al. Exploring the mechanism of Danggui Buxue decoction against acute renal insufficiency using network pharmacology and molecular docking. Molecular & Cellular Biomechanics. 2024; 21(3): 388. https://doi.org/10.62617/mcb388

**ARTICLE INFO**

Received: 18 September 2024
Accepted: 11 November 2024
Available online: 25 November 2024



**Abstract:** The Danggui Buxue decoction (DGBX), consists of Angelica sinensis (Oliv.) Diels, and Astragalus membranaceus (Fisch.) Bunge is known to replenish the blood. However, the mechanisms underlying acute renal injury (ARI) as caused by DGBX are still unclear. Therefore, we aimed to investigate the pharmacological effects of DGBX using a mouse model induced by 1% $HgCl_2$. The key components were selected based on an assessment of gastrointestinal absorption potential and drug-likeness characteristics utilizing the SwissADME tool. The core chemical compositions were screened using Gene Ontology (GO) functional analysis and possible signaling pathways were identified through pathway enrichment analysis. After protein-protein interaction (PPI) analysis, a "herb-ingredient-target" network was established via target gene prediction of the DGBX and ARI. Finally, molecular docking was performed to determine the binding affinity between the active ingredients and disease targets. DGBX significantly reduced renal index and serum levels of blood urea nitrogen (BUN), and creatinine (CRE) in mice administered with 1% $HgCl_2$. Network pharmacology analysis identified 3,9-di-O-methylnissolin, (6aR,11aR)-9,10-dimethoxy-6a, 11a-dihydro-6H-benzofurano[3,2-c] chromen-3-ol, (3R)-3-(2-hydroxy-3,4-dimethoxyphenyl) chroman-7-ol, jaranol, kaempferol, and 7-O-methylisomucronulatol as the six core ingredients of DGBX. Epidermal Growth Factor Receptor (EGFR), RAC-alpha Serine/Threonine-ProteinKinase1(AKT1), Phosphoinositide-3-Kinase Catalytic Subunit Alpha (PIK3CA), Src homology 2 domain-containing tyrosine kinase (SRC), Mitogen-Activated Protein Kinase1(MAPK1), and Estrogen Receptor1(ESR1) were selected as the six effective core targets. Furthermore, molecular docking revealed that the six core ingredients interacted well with six primary targets. The components of DGBX, including A sinensis (Oliv.) Diels and A membranaceus (Fisch.) Bunge may treat ARI by affecting the expression of EGFR, AKT1, PIK3CA, SRC, MAPK1, and ESR1.

**Keywords:** Danggui Buxue decoction; acute renal insufficiency; network pharmacology; molecular docking

## 1. Introduction

Acute renal injury (ARI) is a clinical condition resulting from a sudden and temporary decrease in renal function, a variety of factors can trigger ARI and it occurs within a short period. The factors that drive the development of ARI include decreased glomerular filtration rate, retention of nitrogen products (such as creatinine and urea nitrogen), water, electrolyte and acid-base balance disorders, and multiple system syndrome in severe cases [1,2]. In the context of nephrology, ARI is common condition that has been shown to pose a significant risk to the life and well-being of

patients [3]. In traditional chinese medicine (TCM), ARI falls under the classification of "retention of urine", and its treatment entails clearing heat and diuresis, thereby detoxifying and tonifying the kidney [4].

In-depth research on Traditional Chinese Medicines (TCM) has recently gained increasing attention [5]. Danggui Buxue decoction (DGBX) is composed of *Angelica sinensis* (Oliv.) Diels and *Astragalus membranaceus* (Fisch.) Bunge, was first recorded in "On the Differentiation of Internal and External Injuries" [6], and it can nourish the blood [7]. DGBX also plays a significant role in blood formation [8] and the modulation of the immune system [9], cardiovascular system protection [10], and blood lipids regulation [11]. According to the traditional Chinese medicine theory, the primary cause of chronic kidney disease is qi deficiency and blood stagnation. Hence, future research should focus on the treatment approach of fortifying qi and enriching blood to enhance renal function and postpone renal fibrosis. Danggui Buxue Decoction, a renowned formula for reinforcing qi and nourishing blood, is frequently prescribed in clinical practice [12]. Preliminary studies have validated its efficacy in combating renal failure [13].

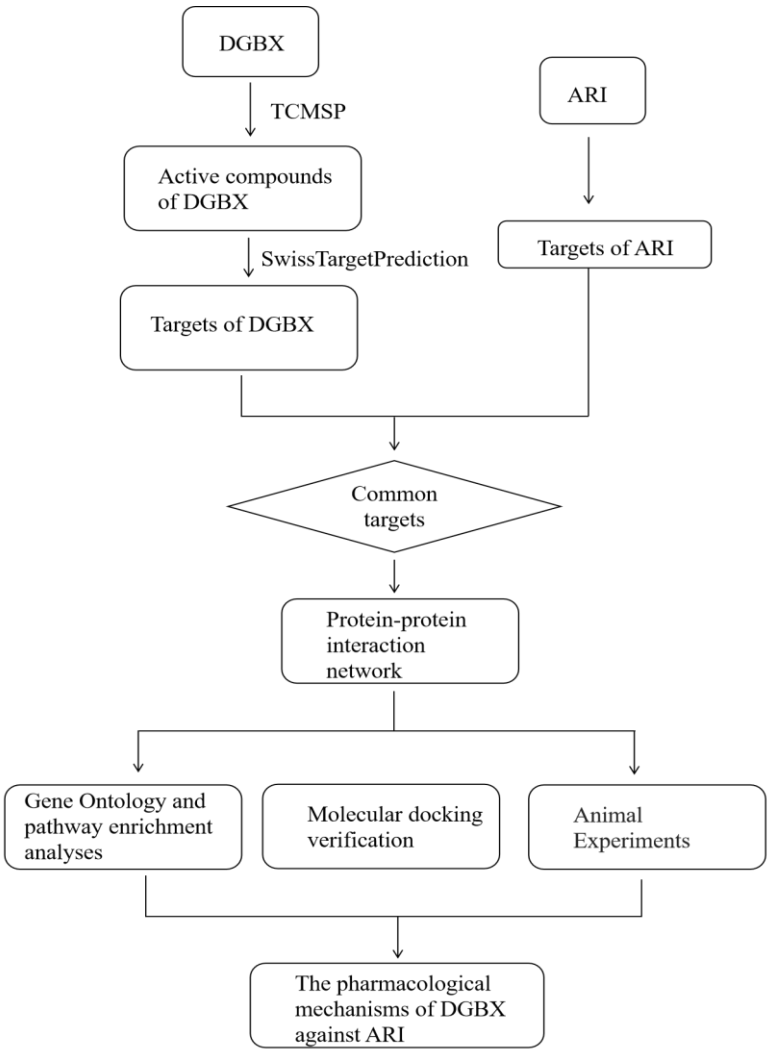


**Figure 1.** The workflow of the current study.

The composition of TCM is complex; and it is mostly used in compound form, and its therapeutic effect may involve a variety of biomolecular mechanisms. However, only a few mechanisms of action have been fully elucidated, which is a core issue that must be resolved for the sustainable development of TCM [14]. To investigate the intricate connection between herbs and diseases, network pharmacology is employed to construct a "herbs-target-disease" network and enabling the exploration of regulatory mechanisms on diseases. This approach may reveal the underlying mechanisms of action of drugs in disease treatment [15]. In this study, we used a $HgCl_2$-induced mouse model to investigate the pharmacological effects of DGBX on ARI. Furthermore, effective constituents and putative targets of DGBX for addressing ARI were predicted using network pharmacology and the underlying mechanisms were analyzed. Finally, the binding patterns and affinities of the molecules were confirmed using molecular docking. The study process is illustrated in **Figure 1**.

## 2. Materials and methods

### 2.1. Reagents and chemicals

*A. sinensis* (Oliv.) Diels and *A. membranaceus* (Fisch.) Bunge was purchased from Beijing Tongrentang (Anguo) Traditional Chinese Medicine Pieces Co., Ltd. (Beijing, China), with batch numbers ZY2207049 and ZY00250201 respectively, the medicinal parts of both *A. sinensis* and *A. membranaceus* are their roots. Bailing (BL) capsules were obtained from Sino-American East China Pharmaceutical Co., Ltd. (Hangzhou, China), $HgCl_2$ solution (1%) was obtained from the experimental center of Sanquan College of Xinxiang Medical College, Blood urea nitrogen (BUN) and creatinine (CRE) assay kits were purchased from Nanjing Jiancheng Haihao Biotechnology Co., Ltd. (Nanjing, China) with production batch numbers 20230313 and 20230322 respectively.

### 2.2. Preparation of DGBX

Firstly, 250 g of A *membranaceus* and 50 g of A *sinensis* were soaked in 2400 mL of distilled water for 60 min, heated to boiling,then decocted for 30 min, and filtered through a gauze. Next, the filter residue was boiled in 1800 mL distilled water and then filtered. The filtrate was mixed twice, and evaporated to 187.5 mL at 60–65 °C. Then, the final concentration of DGBX was 1.6 g/mL, and the herb was stored at 4 °C.

### 2.3. Animals

Kunming mice (male, 6–8 weeks of age) were obtained from Beijing Vital River Laboratory Animal Technology Co., Ltd. (Beijing, China). The experimental procedures for animals were approved by the Ethics Committee of the Experimental Animal Platform of Zhengzhou University School of Medical Sciences. The ethics approval number for this experiment is ZZU-LAC20230324. The animals were raised at the Experimental Animal Platform of Zhengzhou University School of Medical Sciences. During the experiment, mice were housed in cages with unrestricted access

to water and food. The temperature was maintained at 20–25 °C, and the humidity was 50–60 %.

## 2.4. Mice models of ARI and experimental procedures

After seven days of adaptive feeding, 72 mice were randomly divided into six groups: Control, $HgCl_2$, $HgCl_2$ + BL, $HgCl_2$ + DGBX-L, $HgCl_2$ + DGBX-M, $HgCl_2$ + DGBX-H. Briefly, the mice in the $HgCl_2$ + BL, $HgCl_2$ + DGBX-L, $HgCl_2$ + DGBX-M, and $HgCl_2$ + DGBX-H groups received BL (2.0 g/kg), DGBX (0.3 g/ mL), DGBX (0.6 g/mL), and DGBX (1.6 g/mL), respectively, by intragastric administration. Fifteen minutes later, the mice in the last five groups receiving $HgCl_2$ were injected with 1% $HgCl_2$ (5 mg/kg) dissolved in saline into the thigh muscle, A similar procedure was carried out on the control group mice, wherein saline was injected into the same site.After 1% $HgCl_2$ administration for 6, 24 and 48h, the mice were sacrificed and serum was collected for further analysis [16].

### 2.4.1. Renal index analysis

The kidney tissues were collected and weighed. The renal index was calculated as follows: [bilateral renal wet weight/body weight] × 100.

### 2.4.2. Measurement of serum creatinine and blood urea nitrogen content

Serum was collected for the analysis of CRE and BUN levels using related assay kits according to the manufacturer's instructions.

### 2.4.3. Collection of active ingredients of DGBX and disease targets related to ARI

Traditional Chinese Medicine Systems Pharmacology Database and Analysis Platform(TCMSP) (https://old.tcmsp-e.com/tcmsp.php) and SwissADME databases (http://www.swisstargetprediction.ch/) were used to identify potential active ingredients. The constituents with high gastrointestinal (GI) absorption (OB ≥ 30%) and more than 0.18 in drug-likeness (DL) analysis were selected as potential active ingredients [17–19]. Disease targets related to ARI were obtained from Disgenet (https://disgenet.com/) and GeneCards (https://www.genecards.org/). The disease targets related to ARI were selected in Disgenet using "Summary of Gene-Disease Associations" and GeneCards according to Relevance score ≥ 5.2 both after searching "acute renal insufficiency" as keywords. Target genes were combined from the two databases and duplicates were removed.

### 2.4.5. The intersection between active ingredients of DGBX and gene targets related to ARI

Potential targets of DGBX to treat ARI were obtained by intersecting the active component targets of DGBX with the targets related to ARI using the Venny 2.1.0 platform (https://bioinfogp.cnb.csic.es/tools/venny/).

### 2.4.6. Protein-protein interaction network construction

To better understand the protein-protein interactions (PPIs) involving the target genes, the selected potential targets were queried in the STRING database (https://string-db.org). *Homo sapiens* was selected for the analysis.The data that were

saved, were imported into Cytoscape 3.9.1 (https://cytoscape.org/); from this analysis, core targets were identified based on the degree value.

The highest confidence level was set at a medium confidence > 0.9, and the unconnected nodes were hidden. The greater the centrality of a node, the greater its importance in the constructed network [20,21].

#### 2.4.7. GO analysis of core targets andKyoto Encyclopedia of Genes and Genomes (KEGG) signaling pathway enrichment

The DAVID database (https://david.ncifcrf.gov) was used to perform GO analysis and enrich the KEGG signaling pathways for targets. The species and background were set as "Homo sapiens" [22–24]. Differences were considered statistically significant at $p < 0.05$. The top ten pathways of biological process, cell component, and molecular functions were subjected to GO enrichment analysis. The length of the columns in the obtained GO analysis histogram is related to the number of enriched differential genes. The greater the number of differential genes, the longer the histogram length. Through KEGG enrichment analysis, signaling pathways enriched by the common targets of DGBX and ARI were obtained. The visual bubble map was processed using the bioinformatics website (https://www.bioinformatics.com.cn/). The smaller the *p*-value, the larger and darker the bubbles in the bubble map.

#### 2.4.8. Drug-target-pathway-disease network construction

The "Herbs-key ingredients", "key ingredients-core targets", and "disease-core targets" were inserted into Cytoscape 3.9.1 for the purpose of constructing the "DGBX-targets-pathway-ARI" network. Common key targets were obtained by comparing the obtained target with the key targets of the PPI network and were then used for the next molecular docking steps.

### 2.5. Molecular docking

The molecular docking process was performed using AutoDock Vina software v1.5.6, which is accessible at https://vina.scripps.edu. The grid box parameters were set to 126 × 124 × 126 and centered at (2.67, −19.932, 8.838), which covered all pocket-binding positions. Crystal protein structures were obtained from the Protein Data Bank (https://www.uniprot.org/), and the details of the protein targets were as follows: AKT1 (PDB ID: 1UNQ), EGFR (PDB ID: 5HG8), ESR (PDB ID: 2CBP), SRC (PDB ID: 1FMK), MAPK1 (PDB ID: 6SLG), and SRC (PDB ID: 7L1C). The inhibitor ligands and water were removed from the protein structures, and polar hydrogen atoms were added to the protein structures for completeness [25–27]. It is generally considered that a binding energy of ≤ −5.0 kcal/mol indicates effective ligand-receptor binding, while a binding energy of ≤ −7.0 kcal/mol signifies strong binding activity. The AutoDock results were inserted into Python-Pymol software (https://pymol.org/2/), and receptor and ligand binding was visualized [28].

### 2.6. Statistical methods

Data are presented as mean ± standard deviation. GraphPad Prism 8.0 and Excel software were used for analyzing statistics. The differences were compared via one-way ANOVA among groups, and $p < 0.05$ were considered significant at $p < 0.05$.

## 3. Results

### 3.1. DGBX reduced renal index in ARI mice

The renal index was estimated to investigate the effect of DGBX on renal edema. Compared with the blank control group, $HgCl_2$ treatment obviously caused a higher renal index, especially at 24 and 48 h ($p < 0.0001$ vs control group). Renal index levels in the DGBX- treated groups showed a significant decrease at 24 h ($p < 0.05$ and $p < 0.01$ respectively vs the $HgCl_2$ group) and 48 h ($p < 0.05$ and $p< 0.0005$, respectively, vs $HgCl_2$ group) compared with the $HgCl_2$-treated mice (**Figure 2**). Taken together, we concluded that DGBX could prevent renal edema in $HgCl_2$-induced ARI mice.

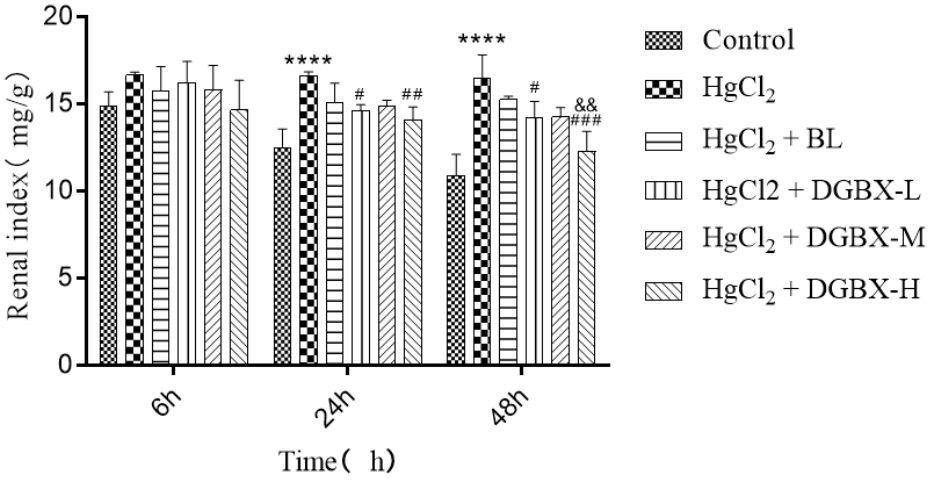


**Figure 2.** DGBX reduced renal index in ARI mice.

Note: $n = 12$, ****$p < 0.0001$ vs. control group; $^{\#}p < 0.05$, $^{\#\#}p < 0.01$, and $^{\#\#\#}p < 0.0005$ vs. $HgCl_2$ group; $^{\&\&}p < 0.01$ vs. BL group.

### 3.2. DGBX reduced serum BUN and CRE content in ARI mice

We examined the effects of DGBX on renal function in $HgCl_2$-induced ARI mice. With the extension of $HgCl_2$ stimulation time, the level of serum BUN in mice increased significantly at 6, 24, and 48 h ($p < 0.0001$ vs. control group) in the $HgCl_2$ group with statistical significance ($p < 0.0001$) compared to the control group. This finding demonstrated that the content of the serum BUN content was inhibited by DGBX treatment, especially in the high-dose group at 6 ($p < 0.0005$ vs. $HgCl_2$ group), 24 ($p < 0.0001$ vs. $HgCl_2$ group), and 48 h ($p < 0.0001$ vs. $HgCl_2$ group) (**Figure 3**). In addition to serum BUN levels, serum CRE levels were evaluated. The increasing trend in serum CRE and BUN levels was consistent at 6, 24 and 48 h ($p < 0.0001$ vs. control group). DGBX treatment led to a dose-dependent increase in serum CRE levels, with the effect being statistically significant. ($p < 0.0001$ vs. $HgCl_2$ group) (**Figure 4**). These results indicated that DGBX improved renal function in $HgCl_2$-induced ARI mice.

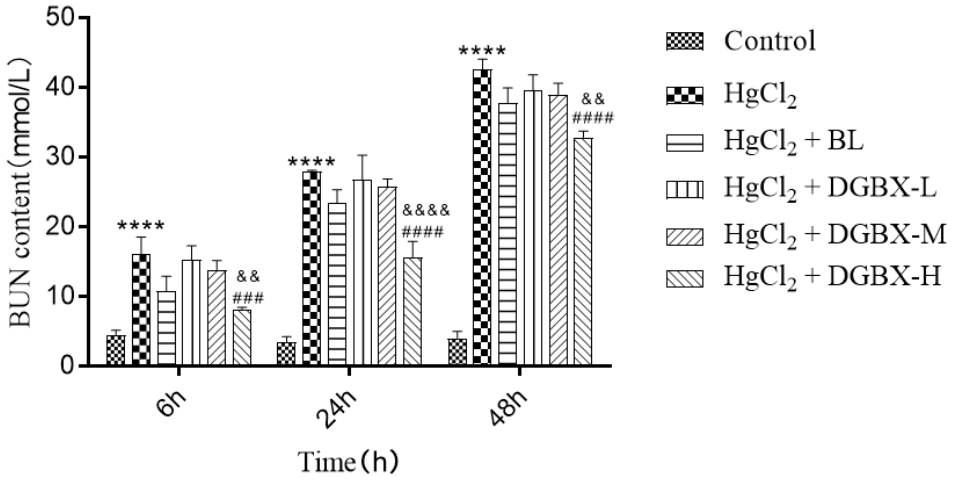


**Figure 3.** DGBX reduced serum BUN content in ARI mice.

Note: $n = 12$, ****$p < 0.0001$ vs. control group; $^{\#}p < 0.05$, $^{\#\#\#}p < 0.0005$, and $^{\#\#\#\#}p < 0.0001$ vs. $HgCl_2$ group; $^{\&\&}p < 0.001$ vs. BL group.

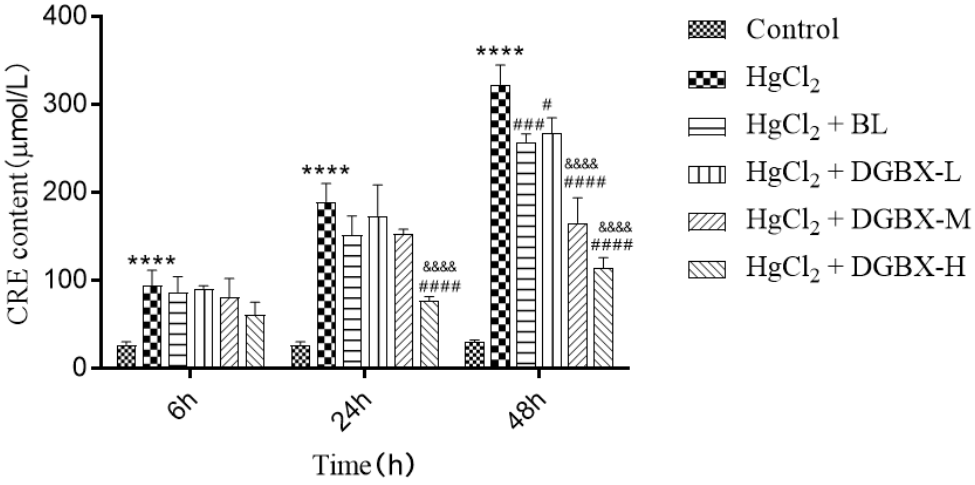


**Figure 4.** DGBX reduced serum CRE content in ARI mice.

Note: $n = 12$; ****$p < 0.0001$ vs. control group; $^{\#}p < 0.05$, $^{\#\#\#}p < 0.0005$, and $^{\#\#\#\#}p < 0.0001$ vs. $HgCl_2$ group; $^{\&\&\&}p < 0.0001$ vs. BL group.

## 3.3. Screening active ingredients in DGBX

The standard cutoffs ("Oral bioavailability" [OB] ≥ 30% and "Drug likeness" [DL] ≥ 0.18) were used to screen for the active ingredients of drugs using SwissADME and TCMSP. To identify the active ingredients of DGBX, the PubChem and SwissTargetPrediction databases were used to obtain, 20 active components in Astragalus and Angelica (**Table 1**).

**Table 1.** Effective components screened from DGBX.

| Drug | Mol ID | Molecule Name | OB (%) | DL |
|---|---|---|---|---|
| Angelica sinensis | MOL000211 | Mairin | 55.38 | 0.78 |
| | MOL000239 | Jaranol | 50.83 | 0.29 |

**Table 1.** (*Continued*).

| Drug | Mol ID | Molecule Name | OB (%) | DL |
|---|---|---|---|---|
| | MOL000033 | (3S,8S,9S,10R,13R,14S,17R)-10, 13-dimethyl-17-[(2R,5S)-5-propan-2-yloctan-2-yl]-2,3,4,7,8,9,11,12,14,15,16,17-dodecahydro-1H-cyclopenta[a]phenanthren-3-ol | 36.23 | 0.78 |
| | MOL000354 | isorhamnetin | 49.60 | 0.31 |
| | MOL000371 | 3,9-di-O-methylnissolin | 53.74 | 0.48 |
| | MOL000374 | 5'-hydroxyiso-muronulatol-2',5'-di-O-glucoside | 41.72 | 0.69 |
| | MOL000378 | 7-O-methylisomucronulatol | 74.69 | 0.30 |
| | MOL000379 | 9,10-dimethoxypterocarpan-3-O-β-D-glucoside | 36.74 | 0.92 |
| | MOL000380 | (6aR,11aR)-9,10-dimethoxy-6a,11a-dihydro-6H-benzofurano[3,2-c] chromen-3-ol | 64.26 | 0.42 |
| | MOL000387 | Bifendate | 31.10 | 0.67 |
| | MOL000392 | formononetin | 69.67 | 0.21 |
| | MOL000417 | Calycosin | 47.75 | 0.24 |
| | MOL000422 | kaempferol | 41.88 | 0.24 |
| | MOL000433 | FA | 68.96 | 0.71 |
| | MOL000438 | (3R)-3-(2-hydroxy-3,4-dimethoxyphenyl) chroman-7-ol | 67.67 | 0.26 |
| | MOL000439 | isomucronulatol-7,2'-di-O-glucosiole | 49.28 | 0.62 |
| | MOL000442 | 1,7-Dihydroxy-3,9-dimethoxy pterocarpene | 39.05 | 0.48 |
| | MOL000098 | quercetin | 46.43 | 0.28 |
| Astragalus membranaceus | MOL000358 | beta-sitosterol | 36.91 | 0.75 |
| | MOL000449 | Stigmasterol | 43.83 | 0.76 |

### 3.4. Screening of DGBX chemical ingredient targets and ARI targets

SwissTargetPrediction, TCMSP, and PubChem were used to identify drug targets. We identified 432 targets genes for the 20 compounds in DGBX, after removing duplicates. Additionally, 927 disease targets were identified in the GeneCards and Disgenet databases. A total of 99 overlapping targetswere uncovered via using VENNY 2.1 software to cross the DGBX-related targets with ARI-related targets (**Figure 5**).

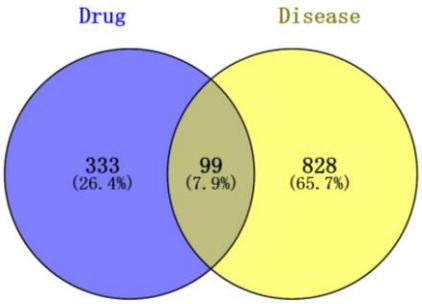


**Figure 5.** Venn diagram of related targets of DGBX-ARI.

### 3.5. Constructing the herb-ingredient-target network

The "herb-ingredient-target" network of 121 nodes (2 herbs, 20 ingredients, and 99 targets) and 364 edges was established (**Figure 6**). Components with a relatively high degree included 3,9-di-O-methylnissolin, (6aR,11aR)-9,10-dimethoxy-6a, 11a-dihydro-6H-benzofurano[3,2-c] chromen-3-ol, (3R)-3-(2-hydroxy-3, 4-dimethoxyphen-yl) chroman-7-ol, jaranol, kaempferol, and 7-O-methylisomucronulatol. This suggests that these compounds might be potential active constituents of DGBX in addressing ARI (**Table 2**).

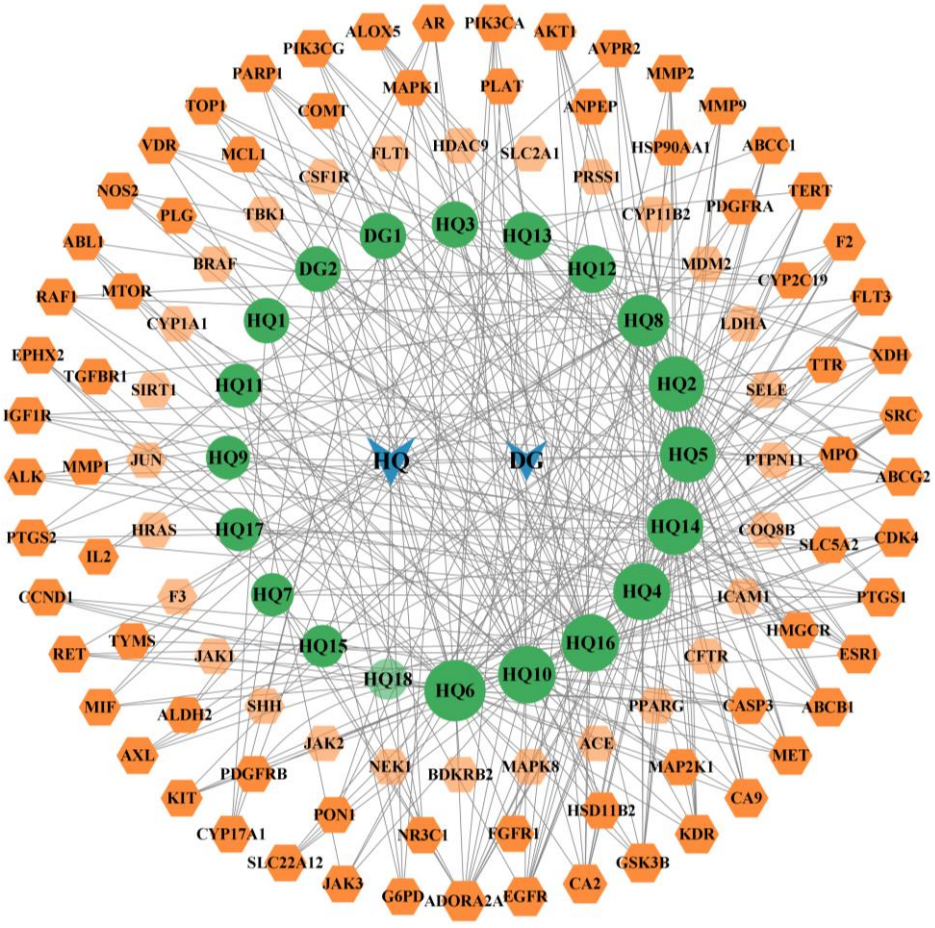


**Figure 6.** The network of herb-ingredient-target network.

**Table 2.** Core active components of DGBX in treatment of acute renal insufficiency.

| name | MOL ID | Molecule Name | Degree | Betweenness Centrality | Closeness Centrality |
|---|---|---|---|---|---|
| HQ6 | MOL000371 | 3,9-di-O-methylnissolin | 41 | 0.27 | 0.45 |
| HQ10 | MOL000380 | (6aR,11aR)-9,10-dimethoxy-6a,11a-dihydro-6H-benzofurano[3,2-c] chromen-3-ol | 34 | 0.13 | 0.43 |
| HQ16 | MOL000438 | (3R)-3-(2-hydroxy-3, 4-dimethoxyphenyl) chroman-7-ol | 34 | 0.14 | 0.42 |
| HQ4 | MOL000239 | Jaranol | 33 | 0.12 | 0.44 |
| HQ14 | MOL000422 | kaempferol | 32 | 0.09 | 0.43 |
| HQ8 | MOL000378 | 7-O-methylisomucronulatol | 23 | 0.10 | 0.40 |

### 3.6. PPI network analysis

To construct a PPI network reflecting the interaction between DGBX and ARI, 99 herb-disease overlapping targets identified through the Venn diagram (**Figure 5**) were introduced into the STRING database and visualized using Cytoscape 3.9.1 (**Figure 7**).

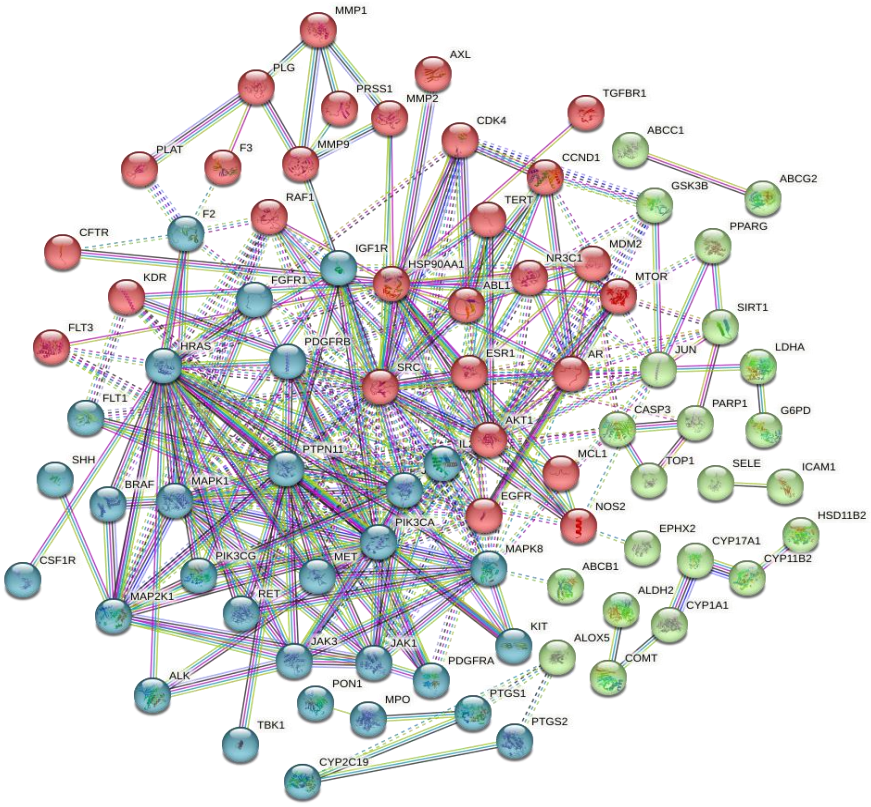


**(A)**

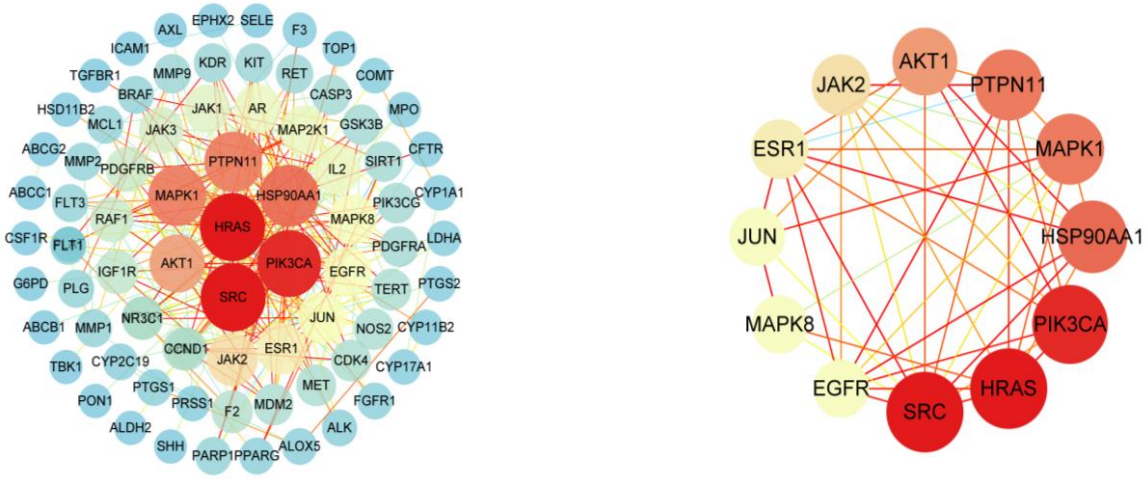


**(B)** **(C)**

**Figure 7.** Protein-protein interaction (PPI) network of overlapping targets between drug and disease, **(A)** initial PPI network; **(B)** optimize PPI network; **(C)** core PPI network.

The average value of the degree of centrality was 6.85, and, the key targets were defined as whose degree value was 2 times higher than the average. The top 12 potential targets were selected as the core targets, which included HRAS, SRC, PIK3CA, PTPN11, MAPK1, MAPK8, HSP90AA1, AKT1, JAK2, ESR1, EGFR and JUN (**Table 3**).

**Table 3.** PPI core target.

| name | Degree | name | Degree |
|---|---|---|---|
| SRC | 28 | AKT1 | 20 |
| HRAS | 28 | JAK2 | 16 |
| PIK3CA | 27 | ESR1 | 15 |
| HSP90AA1 | 23 | MAPK8 | 14 |
| PTPN11 | 22 | EGFR | 14 |
| MAPK1 | 22 | JUN | 14 |

## 3.7. GO and KEGG pathway enrichment analysis

To explore the dynamic processes of DGBX in ARI, we employed the DAVID database to analyze the GO bioprocesses (biological processes [BPs], molecular functions [MFs], and cellular components [CCs]) of the 12 core targets (**Figure 8**).

The analysis identified the top 10 biological processes BPs related to DGBX treatment involved were signal transduction mechanisms, cellular reactions to reactive oxygen species, cellular response to cadmium ions, epidermal growth factor receptor signaling pathway, the enhancement of ERK1 and ERK2 cascade, T cell co-stimulation, and the facilitation of nitric oxide biosynthetic process, augmentation of fibroblast proliferation, cellular response to mechanical stimulus, and positive regulation of peptidyl-serine phosphorylation. The main CC enrichment was in the cytosol, cytoplasm, nucleoplasm, plasma membrane, macromolecular intricate structure, mitochondrion compartment, and the cytoplasmic area surrounding the nucleus, and focal adhesioneuchromatin, et al. The MFs were primarily associated

with adenosine triphosphate(ATP), binding of identical proteins, enzymatic binding, kinase binding specificity regulatory function of nitric oxide synthase, kinase enzymatic activity, interaction with ubiquitin protein ligases, protein kinase enzymatic action, binding affinity for insulin receptor substrate and ATPase interaction.

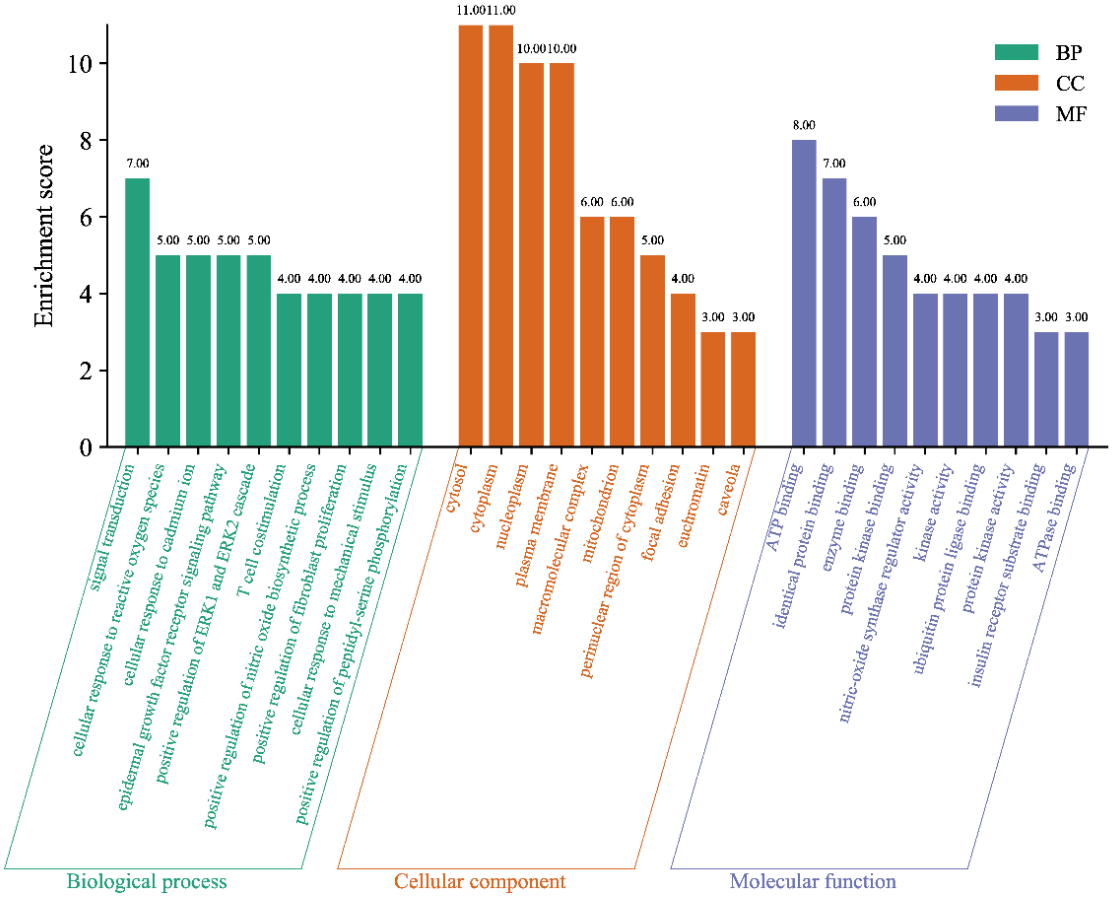


**Figure 8.** GO enrichment analysis.

To predict the possible mechanisms underlying the effectiveness of the herbal remedies, the 12 crucial genes identified through PPI analysis were submitted to the DAVID database for enrichment analysis of the KEGG pathway.

Under a threshold of $p < 0.01$, 95 pathways were identified for the herbal anti-ARI effects. The top 10 related pathways included endocrine resistance, chemical carcinogenesis-receptor activation, prolactin signaling pathway, estrogen signaling pathway, ErbB signaling pathway, PD-L1 expression PD-1 checkpoint pathway in cancer, C-type lectin receptor signaling pathway, lipid and atherosclerosis, chemical carcinogenesis-reactive oxygen species, and relaxin signaling pathway (**Figure 9**). This shows that herbal efficacy is likely related to multiple multiple components and target mechanisms.

The top 10 related pathways identified were endocrine resistance, receptor activation in chemical carcinogenesis, prolactin signaling, estrogen signaling, ErbB signaling, the PD-L1/PD-1 checkpoint pathway in cancer, C-type lectin receptor signaling, lipid metabolism linked to atherosclerosis, reactive oxygen species in chemical carcinogenesis, and the relaxin signaling pathway (**Figure 9**). These findings

suggest that the herbal efficacy can be attributed to its multiple constituents and target mechanisms.

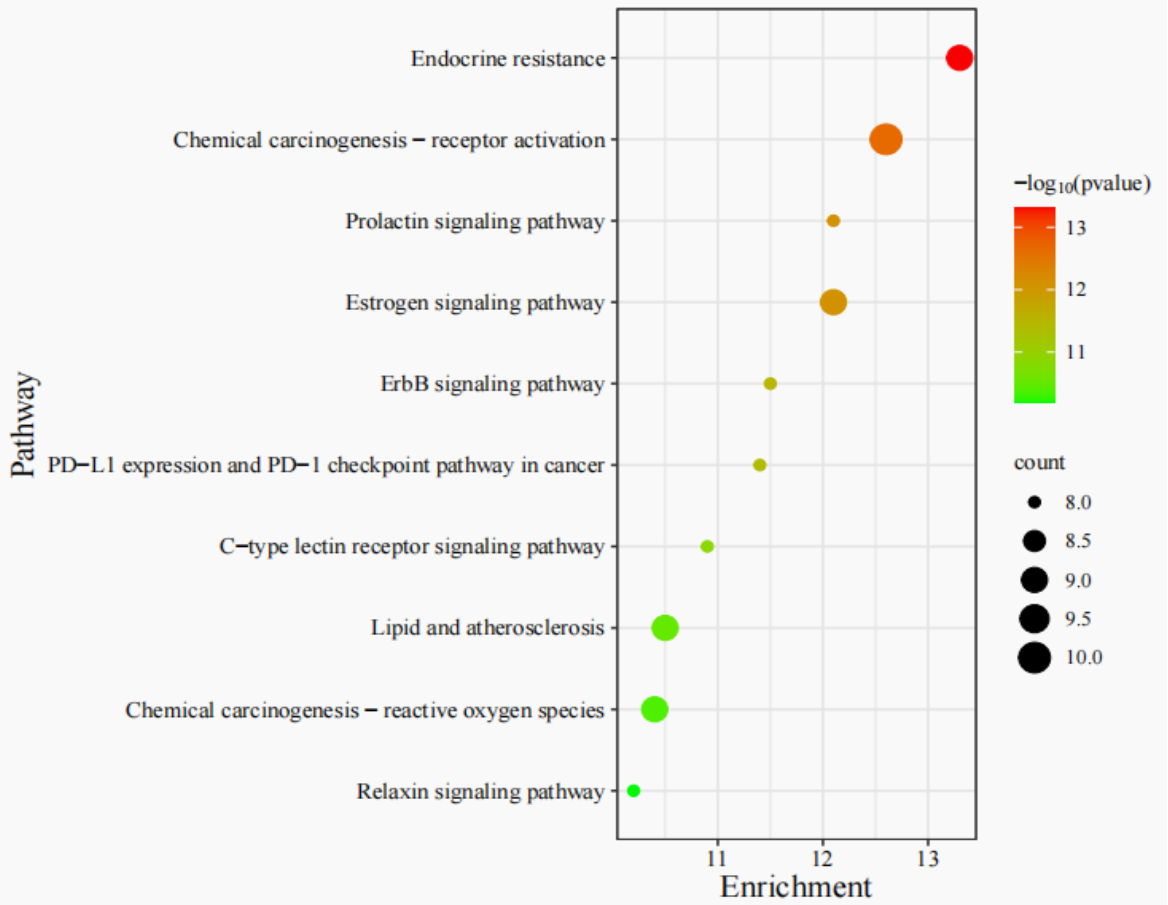


**Figure 9.** KEGG enrichment analysis.

### 3.8. Herbs-target-pathway-diseases network construction

To further clarify the underlying mechanism of DGBX in the treatment of ARI, a more in-depth analysis is necessary. We constructed a herbs-ingredients-targets-disease network of 142 nodes (1 disease, 2 herbs, 20 ingredients, 99 targets and 20 enriched pathways) and 526 edges (**Figure 10**). Nine core targets were identified: GSK3B, AKT1, MAPK1, PIK3CA, EGFR, SRC, ESR1, ADORA2A, and PTGS1. Furthermore, combined with PPI analysis, we discovered that six core targets, including EGFR, AKT1, PIK3CA, SRC, MAPK1, and ESR1, were potential therapeutic targets.

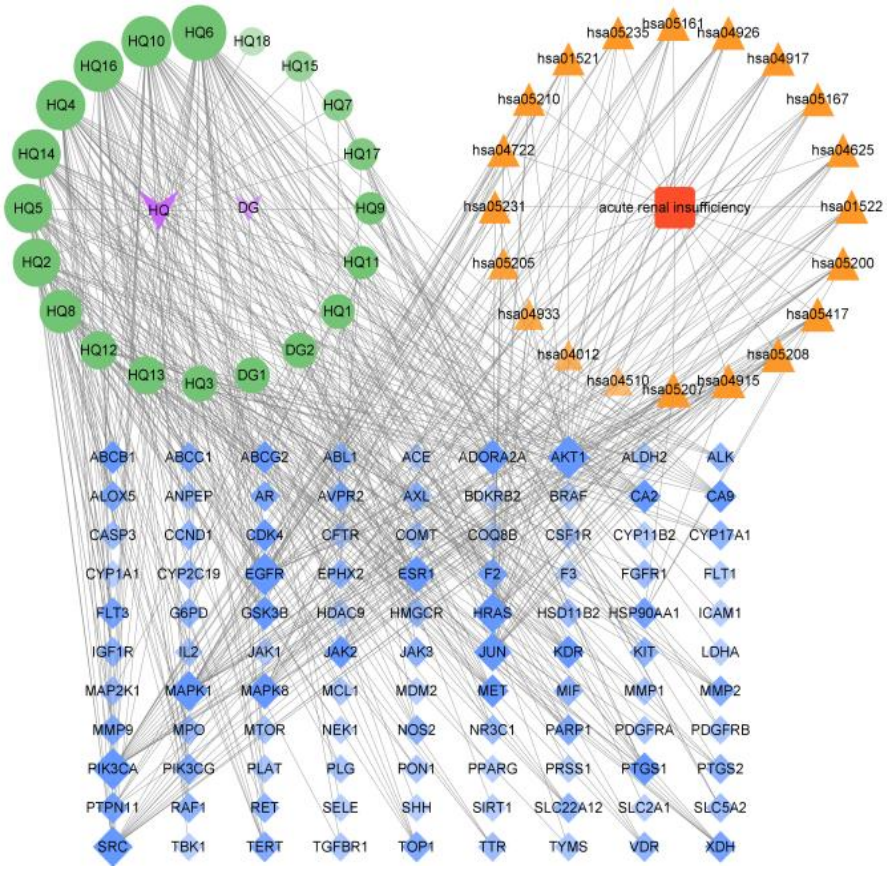


**Figure 10.** Herbs-ingredients-targets-disease network.

## 3.9. Molecular docking

Six core chemical components and six of the core targets were selected as ligands and receptors, respectively. The protein structures of AKT1, EGFR, SRC, PIK3CA, MAPK1, and ESR1 were retrieved from the Protein Data Bank (PDB) (https://www.rcsb.org/), and molecular docking was performed using AutoDock Vina software (**Figure 11)**. After 36 compound-target docking experiments, 13 compound–target pairs showed strong binding activity, and 20 pairs showed weak activity. Thus, we speculated that 91.6% of the active ingredients of DGBX exhibited favorable binding affinity between the active components and the targets of ARI, suggesting that this formula is reasonable and effective for predicting ARI. The molecular docking bond energy heat map is shown in **Figure 12**; and the darker the color, the lower the molecular docking binding energy (**Table 4** and **Figure 12**).

**Table 4.** Docking scores of bioactive compounds with its targets of DGBX.

| Compound | Target | Binding energy （kcal/mol) | Compound | Target | Binding energy (kcal/mol) |
|---|---|---|---|---|---|
| Jaranol | AKT1 | −5.39 | (6aR,11aR)-9,10-dimethoxy-6a,11a-dihydro-6H-benzofurano[3,2-c] chromen-3-ol | AKT1 | −6.22 |
| | EGFR | −7.21 | | EGFR | −7.00 |
| | ESR1 | −4.30 | | ESR1 | −5.50 |
| | SRC | −4.92 | | SRC | −7.32 |
| | MAPK1 | −6.02 | | MAPK1 | −6.35 |
| | PIK3CA | −7.48 | | PIK3CA | −7.67 |

**Table 4.** (*Continued*).

| Compound | Target | Binding energy （kcal/mol) | Compound | Target | Binding energy (kcal/mol) |
|---|---|---|---|---|---|
| 3,9-di-O-methylnissolin | AKT1 | −5.99 | kaempferol | AKT1 | −5.60 |
| | EGFR | −7.45 | | EGFR | −5.88 |
| | ESR1 | −7.23 | | ESR1 | −7.63 |
| | SRC | −7.68 | | SRC | −7.20 |
| | MAPK1 | −6.59 | | MAPK1 | −5.72 |
| | PIK3CA | −6.84 | | PIK3CA | −6.55 |
| 7-O-methylisomucronulatol | AKT1 | −6.11 | (3R)-3-(2-hydroxy-3,4-dimethoxyphenyl) chroman-7-ol | AKT1 | −6.10 |
| | EGFR | −7.07 | | EGFR | −6.69 |
| | ESR1 | −7.84 | | ESR1 | −4.56 |
| | SRC | −6.65 | | SRC | −7.66 |
| | MAPK1 | −6.17 | | MAPK1 | −6.80 |
| | PIK3CA | −5.84 | | PIK3CA | −6.15 |

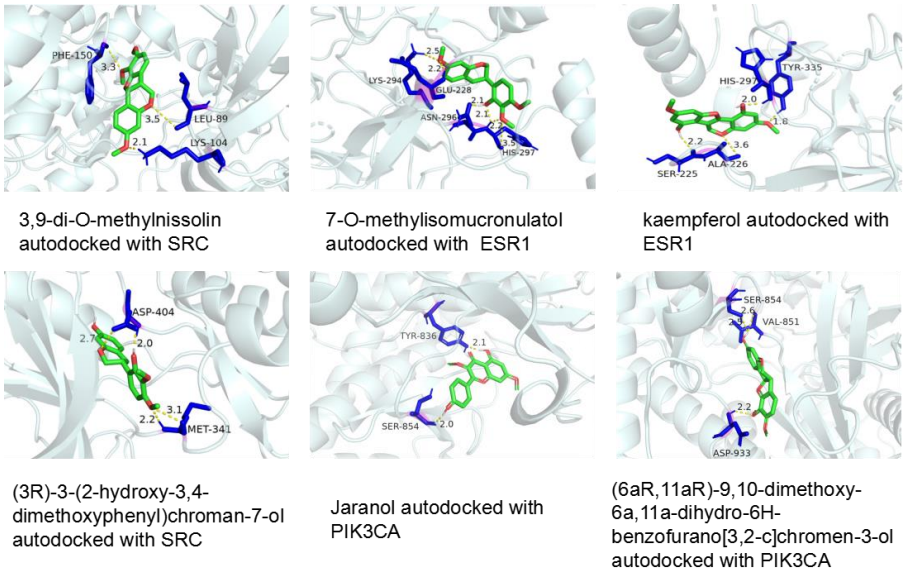


**Figure 11.** Molecular docking pattern.

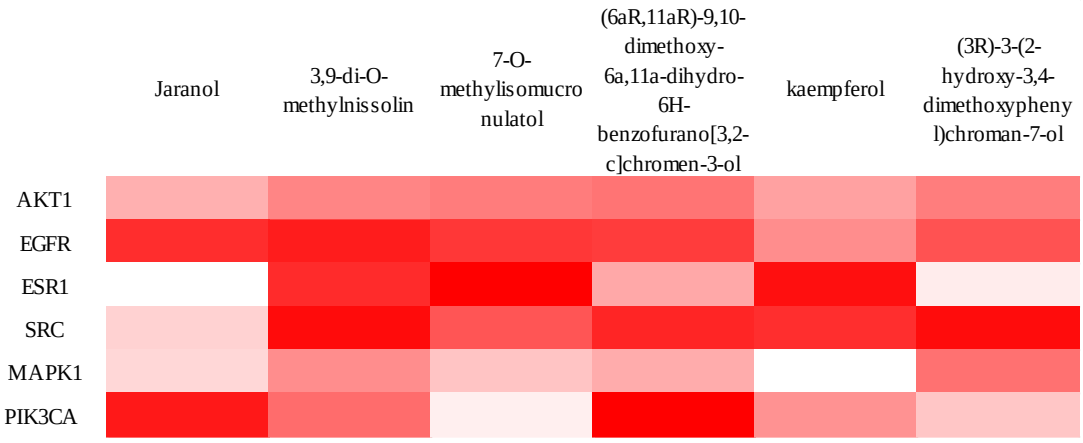


**Figure 12.** Molecular docking bond energy heat map.

## 4. Discussion

Acute renal injury is characterized by a rapid decline in kidney function due to multiple causes and is one of the main life-threatening diseases with a poor prognosis.

Cardiovascular diseases frequently occur alongside acute renal insufficiency, in which a decline in renal function diminishes the effectiveness of cardiovascular treatments and undermines patient outcomes. The combination of *Astragalus membranaceus* and *Angelica sinensis* enhances blood nourishment and circulation, fostering robust qi and blood formation, thereby alleviating an array of symptoms [29]. Danggui Buxue decoction, formulated using these two herbs, is a prominent prescription for addressing qi deficiency and blood stagnation. It has been proven to be highly effective in managing cardiovascular and cerebrovascular disorders, diabetic nephropathy, and other conditions. A study has found that Danggui Buxue Tang (Angelica and Astragalus Decoction) treats diabetic nephropathy by improving inflammation and insulin resistance [30]. Furthermore, some studies have shown that Danggui (Angelica sinensis) and Huangqi (Astragalus membranaceus) can protect the kidney by inhibiting the injuries induced by oxidative stress [31,32].

In this study, we explored DGBX's pharmacological effects on $HgCl_2$-induced ARI *in vivo*, and predicted the probable mechanisms of action utilizing network pharmacology and molecular docking techniques, and found that DGBX ameliorated the renal index, serum BUN, and serum CRE concentrations in a dose-dependent manner. Network analysis identified six core active compounds of DGBX and six potential target genes. Further, Molecular docking analysis demonstrated that 91.6% of the active components of DGBX exhibited good binding activity to the ARI targets.

The "DGBX-ingredients-targets" network demonstrated that the six core active compounds, including 3,9-di-O-methylnissolin, (6aR,11aR)-9,10-dimethoxy-6a, 11a-dihydro-6H-benzofurano[3,2-c] chromen-3-ol,(3R)-3-(2-hydroxy-3,4-dimethoxyphen-yl) chroman-7-ol, jaranol, kaempferol, and 7-O-methylisomucronulatol.

Previous research indicated that jaranol could suppress the expression of reducible adenine dinucleotide phosphoroxidases 2 and 4 mediated by angiotensin II by regulating the atherosclerotic signaling pathway, reducing reactive oxygen species (ROS), and exerting anti-inflammatory effects to protect the kidney [33,34]. Kaempferol has cell membrane protective and antioxidant effects [35]. Previous studies have shown that kaempferol increased Nrf and HO-1 expression to enhance the antioxidant effect, declined ROS generation, and promotes the clearance of reactive oxygen, thereby alleviating oxidative stress in endothelial cells and protecting blood vessels [36,37].

GO enrichment analysis showed that DGBX could act on the perinuclear region of the cytoplasm, mitochondria, plasma membrane, and other organelles; mediate signal transduction and the epidermal growth factor receptor (EGFR) signaling pathway; and exhibit affinity for playing a role in ATP binding, protein binding, enzyme binding, and other processes. Previous studies have demonstrated that EGFR expression is associated with decreased kidney function, associated with the regulated immune reaction during the pathological process of chronic kidney disease [38,39]. Preclinical studies have demonstrated that the EGF receptor, a membrane tyrosine

kinase receptor, is expressed in the kidney and activated after kidney injury [40]. Therefore, it is a promising therapeutic target for kidney injury [38].

The prediction results of KEGG enrichment analysis indicated that DGBX was predominantly associated with endocrine resistance, chemocarcinogenic receptor activation, prolactin signaling pathway, estrogen signaling pathway, and lipid and atherosclerosis metabolic pathways in ARI. DGBX exerts an estrogen-mimicking function in the estrogen signaling pathway [41], related to the repair and regeneration of the kidney via its receptor ESR1, and regulates phosphorus homeostasis through its receptor in the proximal tubule [42].

The "DGBX-target-pathway-ARI" network uncovered that EGFR, AKT1, PIK3CA, SRC, MAPK1, and ESR1 were common targets between DGBX and ARI. These receptors are widely distributed in the body and are involved in cell proliferation, survival, differentiation, and intracellular signaling, *et al* [43,44]. According to the results of molecular docking, 3,9-di-o-methylnissolin and SRC are hydrogen bound to leucine (LEU) at 89, lysine (LYS) at 104 and phenylalanine (PHE) at 150, and the binding energy reaches −7.68. 7-O-methylisomucronulatol and ESR1 bind to glutamic Acid (GLU) at 228 sites, LYS at 294 sites, asparagine (ASN) at 296 sites and histidine (HIS) at 297 sites with hydrogen bonds, and the binding energy reaches -7.84. Kaempferol and ESR1 were hydrogen bonded at serine (SER) at 225, ALA at 226, HIS at 297 and TYR at 335, and the binding energy reached -7.63. (3R)-3-(2-hydroxy-3,4-dimethoxyphenyl) chroman-7-ol and SRC were hydrogen bound to aspartic acid (ASP) at sites 341 and 404 with binding energy of -7.66. (3R)-3-(2-hydroxy-3,4-dimethoxyphenyl) chroman-7-ol and SRC were hydrogen bound to ASP at sites 341 and 404 with binding energy of −7.66. Jaranol and PIK3C were hydrogen bonded at tyrosine (TYR) 836 and SER 854, and the binding energy reached −7.48. (6aR,11aR)-9,10-dimethoxy-6a,11a-dihydro-6H-benzofurano[3,2-c] chromen-3-ol and PIK3C are hydrogen-bonded at VAL 851, SER 854 and ASP 933. The binding energy reaches −7.67. The above binding showed good activity, indicating that the active compounds may play a role in improving renal function through the above target proteins.

AKT1 is associated with renal tubule apoptosis and inflammation, and its absence of AKT1 could aggravate renal injury [45–47]. The AKT family, which consists of three members: (AKT1, AKT2, and AKT3), belongs to the serine/threonine protein kinase family and is intricately interconnected. These proteins play a pivotal role in numerous biological processes. The PI3K/Akt pathway exhibits a robust connection to both inflammatory and anti-inflammatory responses, whereas the Akt signaling pathway can regulate functions such as the generation of inflammatory cytokines and macrophage phagocytosis [48]. Therefore, DGBX inhibits apoptosis in renal tubules and reduces inflammation, which may act on AKT1 targets and protect the kidney. The SRC homologous region 2 domain of SRC contains phosphatase-1 (SHP-1), a key protein that regulates inflammation and immune responses [49]. Deficiency of SHP-1 inhibits gene expression in the PPARα signaling pathway, leading to an increase in ROS and aggravating renal ischemic injury [50,51].

Pre-experimental studies conducted on Kunming mice have shown that administering a 1% $HgCl_2$ solution at a dosage of 1.5 ml/kg effectively induces acute renal insufficiency. The renal index, serum creatinine (CRE) levels, and serum urea

nitrogen (BUN) levels were assessed in the mice. Using a microplate reader and GraphPad Prism 8.0.1 software for data analysis, the renal index and BUN and CRE levels in mouse serum were precisely measured and analyzed. From the perspective of animal experimentation, it has been confirmed that high-dose DGBX (Angelica and Astragalus decoctions) has significant therapeutic benefits in mice with acute renal insufficiency, opening new avenues for the clinical application of DGBX in treating this condition.

## 5. Conclusion

In conclusion, the current study revealed that DGBX significantly protected renal function in an ARI mouse model in a dose-dependent manner. Certain active ingredients in DGBX, including 3,9-di-O-methylnissolin, (6aR,11aR)-9,10-dimethoxy-6a,11a-dihydro-6H-benzofurano[3,2-c]chromen-3-ol, (3R)-3-(2-hydroxy-3,4-dimethoxyphen-yl) chroman-7-ol, jaranol, kaempferol, and 7-O-methylisomucronulatol, influenced ARI pathological process via multiple targets, including EGFR, AKT1, PIK3CA, SRC, MAPK1, and ESR1, and further affected multiple signaling pathways vital for cellular metabolism and apoptosis. Further, in vivo and in vitro are required to confirm this hypothesis.

**Author contributions:** Conceptualization, XL and YM; methodology, JD; software, YL; validation, RL, MS and QZ; formal analysis, XZ; investigation, TH; resources, XL; data curation, XL; writing—original draft preparation, TH; writing—review and editing, TH; visualization, TH; supervision, TH; project administration, XL; funding acquisition, XL. All authors have read and agreed to the published version of the manuscript.

**Funding:** This work was supported by the Natural Science Research Funds of Minhang District, Shanghai [Grant numbers 2023MHZ071].

**Ethical approval:** The animal study protocol was approved by the Institutional Review Board of Academy of Medical Sciences of Zhengzhou University (ZZU-LAC 20230324[19], 2023.01.24).

**Conflict of interest:** The authors declare no conflict of interest.

## References

1. Kellum JA, Romagnani P, Ashuntantang G, Ronco C, Zarbock A, Anders HJ. Acute kidney injury. Nat Rev Dis Primers. 2021;7(1):52. doi:10.1038/s41572-021-00284-z
2. Levey AS, James MT. Acute Kidney Injury. Ann Intern Med. 2017;167(9): ITC66-ITC80. doi:10.7326/AITC201711070
3. USTUNDAG S, SEN S, YALCIN O, et al. L-Carnitine ameliorates glycerol-induced myoglobinuric acute renal failure in rats[J]. Ren Fail, 2009,31(2): 124-133.
4. Mercado MG, Smith DK, Guard EL. Acute Kidney Injury: Diagnosis and Management. Am Fam Physician. 2019;100(11):687-694.
5. Zhong Y, Menon MC, Deng Y, Chen Y, He JC. Recent Advances in Traditional Chinese Medicine for Kidney Disease. Am J Kidney Dis. 2015;66(3):513-522. doi:10.1053/j.ajkd.2015.04.013
6. Gong G, Zhou X, Huang D, et al. Danggui Buxue Tang: A Review of its Major Components. Altern Ther Health Med. 2023;29(5):54-64.

7. Dou Y, Shu Y, Wang Y, et al. Combination treatment of Danggui Buxue Decoction and endothelial progenitor cells can enhance angiogenesis in rats with focal cerebral ischemia and hyperlipidemia. J Ethnopharmacol. 2023; 314:116563. doi:10.1016/j.jep.2023.116563
8. Zhang Y, Yang Y, Ren J, et al. Chinmedomics strategy for elucidating the effects and effective constituents of Danggui Buxue Decoction in treating blood deficiency syndrome. Front Mol Biosci. 2024; 11:1376345. Published 2024 Mar 15. doi:10.3389/fmolb.2024.1376345
9. Jiang X, He Y, Zhao Y, Pan Z, Wang Y. Danggui Buxue Decoction exerts its therapeutic effect on rheumatoid arthritis through the inhibition of Wnt/ β -catenin signaling pathway. J Orthop Surg Res. 2023;18(1):944. Published 2023 Dec 9. doi:10.1186/s13018-023-04439-4
10. Hu G, Yang P, Zeng Y, Zhang S, Song J. Danggui Buxue decoction promotes angiogenesis by up-regulation of VEGFR1/2 expressions and down-regulation of sVEGFR1/2 expression in myocardial infarction rat. J Chin Med Assoc. 2018;81(1):37-46. doi:10.1016/j.jcma.2017.06.015
11. Xue M, Bian Y, Liu Y, et al. Danggui Buxue decoction ameliorates lipid metabolic defects involved in the initiation of diabetic atherosclerosis; identification of active compounds. J Tradit Chin Med. 2020;40(3):414-421. doi:10.19852/j.cnki.jtcm.2020.03.009
12. Song J, Meng L, Li S, Qu L, Li X. A combination of Chinese herbs, Astragalus membranaceus var. mongholicus and Angelica sinensis, improved renal microvascular insufficiency in 5/6 nephrectomized rats. Vascul Pharmacol. 2009 May-Jun;50(5-6):185-93. doi: 10.1016/j.vph.2009.01.005. PMID: 19563735.
13. Zhang L, Wang F, Wang L, Wang W, Liu B, Liu J, Chen M, He Q, Liao Y, Yu X, Chen N, Zhang JE, Hu Z, Liu F, Hong D, Ma L, Liu H, Zhou X, Chen J, Pan L, Chen W, Wang W, Li X, Wang H. Prevalence of chronic kidney disease in China: a cross-sectional survey. Lancet. 2012 Mar 3;379(9818):815-22. doi: 10.1016/S0140-6736(12)60033-6. Erratum in: Lancet. 2012 Aug 18;380(9842):650. PMID: 22386035.
14. Wang J, Wong YK, Liao F. What has traditional Chinese medicine delivered for modern medicine?. Expert Rev Mol Med. 2018;20:e4. Published 2018 May 11. doi:10.1017/erm.2018.3
15. Zhao L, Zhang H, Li N, et al. Network pharmacology, a promising approach to reveal the pharmacology mechanism of Chinese medicine formula. J Ethnopharmacol. 2023;309:116306. doi:10.1016/j.jep.2023.116306
16. Gao D, Zeng LN, Zhang P, et al. Rhubarb Anthraquinones Protect Rats against Mercuric Chloride ($HgCl_2$)-Induced Acute Renal Failure. Molecules. 2016;21(3):298. Published 2016 Mar 8. doi:10.3390/molecules21030298
17. Shang L, Wang Y, Li J, et al. Mechanism of Sijunzi Decoction in the treatment of colorectal cancer based on network pharmacology and experimental validation. J Ethnopharmacol. 2023;302(Pt A):115876. doi:10.1016/j.jep.2022.115876
18. Wang ZY, Li MZ, Li WJ, Ouyang JF, Gou XJ, Huang Y. Mechanism of action of Daqinjiao decoction in treating cerebral small vessel disease explored using network pharmacology and molecular docking technology. Phytomedicine. 2023;108:154538. doi:10.1016/j.phymed.2022.154538
19. Pan L, Peng C, Wang L, et al. Network pharmacology and experimental validation-based approach to understand the effect and mechanism of Taohong Siwu Decoction against ischemic stroke. J Ethnopharmacol. 2022;294:115339. doi:10.1016/j.jep.2022.115339
20. Hunter SA, Cochran JR. Cell-Binding Assays for Determining the Affinity of Protein-Protein Interactions: Technologies and Considerations. Methods Enzymol. 2016;580:21-44. doi:10.1016/bs.mie.2016.05.002
21. Kovács IA, Luck K, Spirohn K, et al. Network-based prediction of protein interactions. Nat Commun. 2019;10(1):1240. Published 2019 Mar 18. doi:10.1038/s41467-019-09177-y
22. The Gene Ontology Consortium. The Gene Ontology Resource: 20 years and still GOing strong. Nucleic Acids Res. 2019;47(D1):D330-D338. doi:10.1093/nar/gky1055
23. Zhu J, Zhao Q, Katsevich E, Sabatti C. Exploratory Gene Ontology Analysis with Interactive Visualization. Sci Rep. 2019;9(1):7793. Published 2019 May 24. doi:10.1038/s41598-019-42178-x
24. Lewis SE. The Vision and Challenges of the Gene Ontology. Methods Mol Biol. 2017;1446:291-302. doi:10.1007/978-1-4939-3743-1_21
25. Ongtanasup T, Kamdenlek P, Manaspon C, Eawsakul K. Green-synthesized silver nanoparticles from Zingiber officinale extract: antioxidant potential, biocompatibility, anti-LOX properties, and in silico analysis. BMC Complement Med Ther. 2024, 24(1):84. doi: 10.1186/s12906-024-04381-w.

26. Ongtanasup T, Prommee N, Jampa O, Limcharoen T, Wanmasae S, Nissapatorn V, Paul AK, Pereira ML, Wilairatana P, Nasongkla N, Eawsakul K. The Cholesterol-Modulating Effect of the New Herbal Medicinal Recipe from Yellow Vine (Coscinium fenestratum (Goetgh.)), Ginger (Zingiber officinale Roscoe.), and Safflower (Carthamus tinctorius L.) on Suppressing PCSK9 Expression to Upregulate LDLR Expression in HepG2 Cells. Plants (Basel). 2022, 11(14):1835. doi: 10.3390/plants11141835.
27. Ongtanasup, T., Tawanwongsri, W., Manaspon, C., Srisang, S., & Eawsakul, K.. Comprehensive investigation of niosomal red palm wax gel encapsulating ginger (Zingiber officinale Roscoe): Network pharmacology, molecular docking, In vitro studies and phase 1 clinical trials. International Journal of Biological Macromolecules, 2024, 277(1): 134334. doi:https://doi.org/10.1016/j.ijbiomac.2024.134334.
28. Zhang S, Zhao YH, Chang ZW, Chen H, Hou HW. Insights into Molecular Mechanism of Nicotine Addiction Based on Network Pharmacology and Molecular Docking Strategy. Journal of Computational Biophysics and ChemistryVol. 2024, 23(01): 35-45. doi:https://doi.org/10.1142/S2737416523500497.
29. Li F, Tang R, Chen LB, Zhang KS, Huang XP, Deng CQ. Effects of Astragalus Combined with Angelica on Bone Marrow Hematopoiesis Suppression Induced by Cyclophosphamide in Mice. Biol Pharm Bull. 2017;40(5):598-609. doi:10.1248/bpb.b16-00802
30. Sun L, Yang Z, Zhao W, Chen Q, Bai H, Wang S, Yang L, Bi C, Shi Y, Liu Y. Integrated lipidomics, transcriptomics and network pharmacology analysis to reveal the mechanisms of Danggui Buxue Decoction in the treatment of diabetic nephropathy in type 2 diabetes mellitus. J Ethnopharmacol. 2022 Jan 30;283:114699. doi: 10.1016/j.jep.2021.114699. Epub 2021 Oct 2. PMID: 34610419.
31. Goto S, Fujii H, Watanabe K, et al. Renal protective effects of astragalus root in rat models of chronic kidney disease. Clin Exp Nephrol. 2023;27(7):593-602. doi:10.1007/s10157-023-02356-8
32. Shahzad M, Small DM, Morais C, Wojcikowski K, Shabbir A, Gobe GC. Protection against oxidative stress-induced apoptosis in kidney epithelium by Angelica and Astragalus. J Ethnopharmacol. 2016;179:412-419. doi:10.1016/j.jep.2015.12.027
33. Song S, Yu J. Integrating Network Pharmacology, Bioinformatics, and Mendelian Randomization Analysis to Identify Hub Targets and Mechanisms of Kunkui Baoshen Decoction in Treating Diabetic Kidney Disease. Curr Pharm Des. 2024;30(42):3367-3393. doi:10.2174/0113816128331463240816145054
34. Liu T, Zhuang XX, Zheng WJ, Gao JR. Integrative Multi-Omics and Network Pharmacology Reveal the Mechanisms of Fangji Huangqi Decoction in Treating IgA Nephropathy. J Ethnopharmacol. Published online October 25, 2024. doi:10.1016/j.jep.2024.118996
35. Park JS, Rho HS, Kim DH, Chang IS. Enzymatic preparation of kaempferol from green tea seed and its antioxidant activity. J Agric Food Chem. 2006;54(8):2951-2956. doi:10.1021/jf052900a
36. Chen Y, Li T, Tan P, et al. Kaempferol From Penthorum chinense Pursh Attenuates Hepatic Ischemia/Reperfusion Injury by Suppressing Oxidative Stress and Inflammation Through Activation of the Nrf2/HO-1 Signaling Pathway. Front Pharmacol. 2022;13:857015. Published 2022 Apr 1. doi:10.3389/fphar.2022.857015
37. Yao H, Sun J, Wei J, Zhang X, Chen B, Lin Y. Kaempferol Protects Blood Vessels From Damage Induced by Oxidative Stress and Inflammation in Association With the Nrf2/HO-1 Signaling Pathway. Front Pharmacol. 2020;11:1118. Published 2020 Jul 22. doi:10.3389/fphar.2020.01118
38. Rayego-Mateos S, Rodrigues-Diez R, Morgado-Pascual JL, et al. Role of Epidermal Growth Factor Receptor (EGFR) and Its Ligands in Kidney Inflammation and Damage. Mediators Inflamm. 2018;2018:8739473. Published 2018 Dec 23. doi:10.1155/2018/8739473
39. Zhang WR, Parikh CR. Biomarkers of Acute and Chronic Kidney Disease. Annu Rev Physiol. 2019;81:309-333. doi:10.1146/annurev-physiol-020518-114605
40. Cao S, Pan Y, Terker AS, et al. Epidermal growth factor receptor activation is essential for kidney fibrosis development. Nat Commun. 2023;14(1):7357. Published 2023 Nov 14. doi:10.1038/s41467-023-43226-x
41. Zhou L, Wong KY, Cao S, et al. A standardized extract of Danggui Buxue Tang decoction selectively exerts estrogenic activities distinctly from tamoxifen. Phytother Res. 2021;35(3):1456-1467. doi:10.1002/ptr.6909
42. Ma HY, Chen S, Du Y. Estrogen and estrogen receptors in kidney diseases. Ren Fail. 2021;43(1):619-642. doi:10.1080/0886022X.2021.1901739

43. Zhao T, Tian Y, Ding X, et al. Genetic Analysis and Targeted Therapy Using Buparlisib and MK2206 in a Patient with Triple Metachronous Cancers of the Kidney, Prostate, and Squamous Cell Carcinoma of the Lung: A Case Report. Onco Targets Ther. 2021;14:2839-2845. Published 2021 Apr 28. doi:10.2147/OTT.S298697
44. Wang Y, Wu D, Wang Y, et al. Bioinformatics study of the potential therapeutic effects of ginsenoside Rh3 in reversing insulin resistance. Front Mol Biosci. 2024;11:1339973. Published 2024 May 23. doi:10.3389/fmolb.2024.1339973
45. Kim IY, Song SH, Seong EY, Lee DW, Bae SS, Lee SB. Akt1 is involved in renal fibrosis and tubular apoptosis in a murine model of acute kidney injury-to-chronic kidney disease transition. Exp Cell Res. 2023;424(2):113509. doi:10.1016/j.yexcr.2023.113509
46. Yufang W, Mingfang L, Nan H, Tingting W. Quercetin-targeted AKT1 regulates the Raf/MEK/ERK signaling pathway to protect against doxorubicin-induced nephropathy in mice. Tissue Cell. 2023;85:102229. doi:10.1016/j.tice.2023.102229
47. Kim IY, Park YK, Song SH, et al. Akt1 is involved in tubular apoptosis and inflammatory response during renal ischemia-reperfusion injury. Mol Biol Rep. 2020;47(12):9511-9520. doi:10.1007/s11033-020-06021-1
48. Grigoryev DN, Liu M, Cheadle C, Barnes KC, Rabb H. Genomic profiling of kidney ischemia-reperfusion reveals expression of specific alloimmunity-associated genes: Linking "immune" and "nonimmune" injury events. Transplant Proc. 2006;38(10):3333-3336. doi:10.1016/j.transproceed.2006.10.129
49. Li N, Lin G, Zhang H, et al. Src Family Kinases: A Potential Therapeutic Target for Acute Kidney Injury. Biomolecules. 2022;12(7):984. Published 2022 Jul 14. doi:10.3390/biom12070984
50. Lizotte F, Rousseau M, Denhez B, et al. Deletion of protein tyrosine phosphatase SHP-1 restores SUMOylation of podocin and reverses the progression of diabetic kidney disease [published correction appears in Kidney Int. 2023 Dec;104(6):1228. doi: 10.1016/j.kint.2023.10.007]. Kidney Int. 2023;104(4):787-802. doi:10.1016/j.kint.2023.06.038
51. Yan S, Sui M, Tian H, et al. Transcriptomic Analysis Revealed an Important Role of Peroxisome-Proliferator-Activated Receptor Alpha Signaling in Src Homology Region 2 Domain-Containing Phosphatase-1 Insufficiency Leading to the Development of Renal Ischemia-Reperfusion Injury. Front Med (Lausanne). 2022;9:847512. Published 2022 May 10. doi:10.3389/fmed.2022.847512